

Arrangement of the Experiment. In this work, a pulsed arrangement of a quasi-isobaric capillary discharge is used as the source of plasma [1]. In this scheme, a stabilized pulse discharge in the vapor of the working body and a discharge with an evaporating wall are combined. The difference from a discharge with an evaporating wall lies in the fact that the material of the wall is not the working body and the pressure arises not as a result of intense evaporation of the wall but is created statistically beforehand in the capillary. The cathode of the discharge is an "infinite" reservoir of liquid working body, which evaporates in the discharge as the discharge burns. Cesium, which has a low ionization potential ($E = 3.87$ eV) and is the optimum substance (of technically practicable materials) for obtaining strong departure from ideality, was chosen as the working body. Estimates for cesium give a Coulombic degree of nonideality $\gamma = e^2 n_e^{1/3} / kT \approx 1$ with $p = 10^8$ Pa and $T = 7000^\circ\text{K}$.

A schematic diagram of the pulsed isobaric source of nonideal plasma with the discharge stabilized by a solid transparent wall is presented in Fig. 1. The main element of the source is the transparent (quartz, glass) capillary 1, hermetically sealed between two electrodes 2. The space underneath the capillary and the capillary itself are loaded with liquid cesium 3 at the beginning of the experiment. A free volume 4, into which the cesium expands during heating, remains above the capillary. The static pressure from an inert gas, which remains virtually constant during the experiment, is applied to the surface of the cesium in the free volume. The cesium located in the capillary is heated up to high temperatures by a sinusoidal current pulse. The possibility of creating a quasistationary, uniform plasma column imposes certain requirements on the organization of the working process in the source. The required electrical power supply and the characteristic time of heating of the plasma are determined by the characteristics of the heat-transfer process and friction in the capillary between the plasma and the wall, as well as by the thermal and gasdynamic inertia of the plasma. The condition for the processes to be isobaric requires that the process not be explosive and that the pressure in the discharge nearly equal the static pressure. It is also necessary that the wall of the capillary does not evaporate strongly or break down.

Estimates of the characteristic discharge time gave a magnitude of the order of 10^{-3} sec. The evaporation temperature of the quartz was estimated from the data in [2] and constitutes $T = 4700^\circ\text{K}$ for $p = 10^8$ Pa. In addition, the evaporating wall reduces the radiation from the discharge at $\lambda = 5 \cdot 10^{-4}$ mm by not less than a factor of 2 [3].

At high temperatures the radiative mechanism of heat transfer predominates in the cesium plasma. The Rosseland mean free path of radiation, estimated using the technique in [4], is presented as a function of temperature for different pressures in Fig. 2 [curves 1-3 correspond to $p = (0.1; 0.5; 1) \cdot 10^8$ Pa]. At low temperatures there should be a tendency for the plasma to be "bleached," i.e., the mean free path length should increase due to the decrease in the probability of the corresponding absorption processes. Thus there should be a minimum of the radiation mean free path in the temperature range $T = (4-6) \cdot 10^3$ K, which can determine the surface brightness of the discharge.

Experimental Setup. In this work, the terminal compression of the walls of the glass capillary is used in order to make sure that the capillary continues to function with internal pressures up to $p = 10^8$ Pa under conditions of high thermal stresses. For this, the capillary sharpened at a 90° angle is clamped through a copper interlayer between two metallic electrodes (see Fig. 1). The terminal forces arising in this case fulfill the role of a "band," which is equivalent to some extent to an external pressure on the capillary. In addition, due to the plasticity of the copper interlayer, the problem of hermetic packing of the capillary is solved at the same time. The fact that there is no need to create an external counter-pressure on the capillary greatly simplified the experimental setup as well as the experimental procedure.

Moscow. Translated from Zhurnal Prikladnoi Mekhaniki i Tekhnicheskoi Fiziki, No. 1, pp. 24-29, January-February, 1984. Original article submitted October 29, 1982.

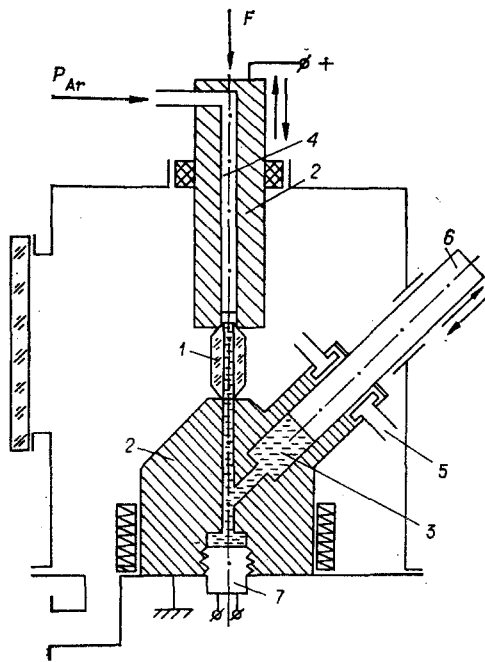


Fig. 1

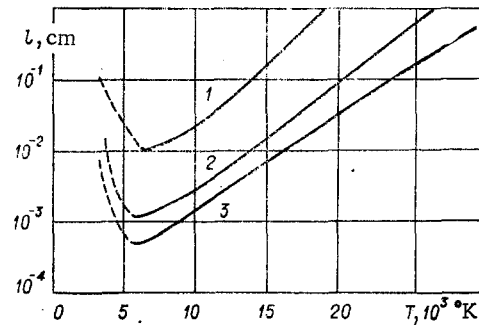


Fig. 2

The setup consists of a protective housing (see Fig. 1), filled with argon up to atmospheric pressure, in which capillaries with a length of $l = 10\text{--}40$ mm and an inner diameter of $d = 0.4\text{--}2$ mm are clamped between the movable electrically insulated electrode at the top and the immobile electrode at the bottom. The clamping force is applied to the top electrode through a dynamometric clamp, calibrated for a force of up to 1000 kg. The top electrode also serves as a means for injecting inert gas at pressures up to 10^8 Pa, created by a booster. The bottom electrode serves to introduce liquid cesium into the capillary by a plunging system 6, which hermetically packs the cesium up to $p = 10^8$ Pa by freezing it in the gap of the plunger pair by means of water cooling 5.

The capillaries are positioned manually with the help of rubber gloves, inserted through two of four portholes in the protective housing. The remaining two portholes are used for observations.

The resistance of the capillary, which varies with time, is less than the resistance of the supply circuits and has little effect on the discharge.

To eliminate extraneous shunting electrical breakdowns, the capillary was clamped through an electrically insulating transparent film with high breakdown voltage. To charge the cesium and initiate the discharge, a small hole was made in the film. Triggering of the electrical circuit and synchronization with high-speed motion picture photography are realized by a special delay block. The magnitude of the voltage drop on the discharge and the discharge current, measured according to the voltage drop on a noninductive shunt, were fixed on an S1-51 electronic storage oscillograph. The discharge time varied in the range $(0.3\text{--}30) \cdot 10^{-3}$ sec and the current varied up to 1200 A. High-speed motion picture photography was performed with a SKS-1M camera with an exposure time of $0.25 \cdot 10^{-3}$ sec. The pressure in the capillary was measured by positioning a piezoelectric quartz LKh-601 sensor in the cavity above the capillary. A high-speed scan of the spectrum of the discharge radiation in time was performed with an ISP-51 spectrograph, to whose holding part a rotating drum was attached. The rate of rotation of the drum and the beginning of the discharge were marked on the film by flashes from a light-emitting diode with a controllable duration.

Experimental Results. The experiments were performed for three values of the initial static pressure $p_0 = (0.25; 0.5; 1) \cdot 10^8$ Pa. Capillaries made of KU brand glass with a 15% content of Na_2O with a diameter of $d = 0.4\text{--}2$ mm and capillaries made of Japanese quartz with a diameter $d = 0.4\text{--}0.7$ mm were used. No differences were observed in the V-A characteristics of the quartz and of the glass with the same geometry and regimes.

The experiments were performed with three characteristic time regimes $3 \cdot 10^{-4}$; $3 \cdot 10^{-3}$; $3 \cdot 10^{-2}$ sec with the leading edge of the current pulse, respectively, equal to 10^{-4} ; $2.5 \cdot 10^{-4}$;

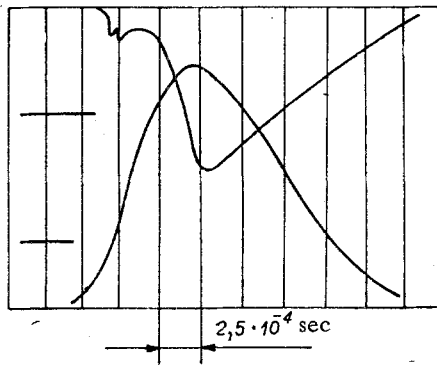


Fig. 3

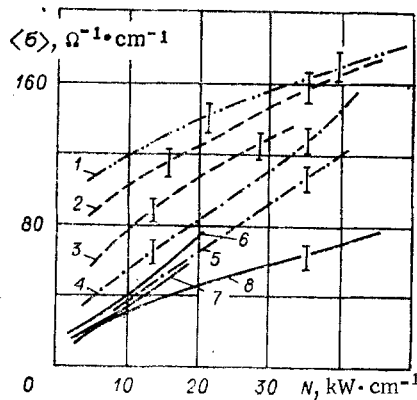


Fig. 4

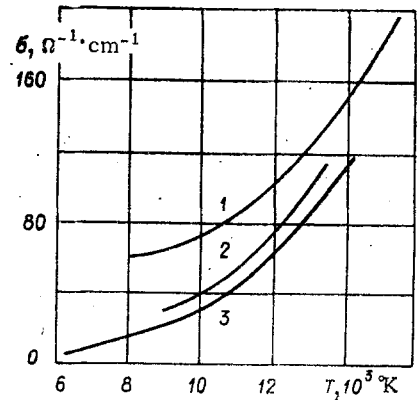


Fig. 5

$5 \cdot 10^{-3}$ sec. The characteristic oscillogram of the V-A characteristics in the time scan regime $\tau = 2.5 \cdot 10^{-4}$ sec/cm for a glass capillary $l = 20$ mm long with a diameter of $d = 2$ mm under a static pressure of $p_0 = 10^8$ Pa is presented in Fig. 3 (voltage at the top and current at the bottom; the meanderings of the calibrations are covered at 500 V and 1000 A). A high-speed synchronous motion picture of the process of ignition and development of the discharge was made. The time for complete filling of the capillary by the discharge corresponds to peak voltage. In the first frames of the motion picture it is evident how the plasma, initiated in the lower end of the capillary, displaces the liquid cesium located above it into the gas volume above the capillary. Then, there follows a complete uniform burning of the discharge and subsequent contraction of the discharge back toward the end. The surface brightness of the discharge remains practically unchanged for different levels of electrical power introduced into the discharge in the experiment. For long discharges ($\tau = 3 \cdot 10^{-2}$ sec) a second voltage peak appears in the V-A characteristic in the region of small currents, which is smoothed out with increasing pressure and diameter of the capillary. For short discharges ($\tau = 3 \cdot 10^{-4}$ sec) there is a strong surge of the current pulse up to the moment that the capillary is ignited and the magnitude of the voltage drop on the capillary during burning of the discharge is higher by 15-20%. As the pressure decreases, the voltage drop on the discharge increases.

Discharge of the plasma out of the capillary is visualized in experiments with a double capillary, in which the discharge is produced only in the lower capillary. The discharge of plasma into the upper capillary, occurring throughout the entire period of complete burning of the capillary, was fixed by high-speed motion picture photography. The discharge velocity, fixed according to the upper boundary of the luminescence, is 10-30 m/sec.

Measurements of the rise of the pressure in the capillary above the static pressure during burning of the discharge showed that the pressure increases smoothly at the beginning stage of burning and then decreases slowly with time. In most of our experiments the excess pressure was $\Delta p = (1.3-1.5) \cdot 10^7$ Pa for a static pressure of $p_0 = 2.5 \cdot 10^7$ Pa and $\Delta p = (0.8-1.3) \cdot 10^7$ Pa for $p_0 = 5 \cdot 10^7$ Pa. A measurement was not performed for $p_0 = 10^8$ Pa. It was established that the pressure drop on the capillary itself is small and that the increase in pressure is related to the heating of the gas cavity $V = 4 \text{ cm}^3$ above the capillary of the plasma flowing into the cavity.

In experiments with shunting of the discharge by an extraneous breakdown, the capillary was extinguished within a time $\tau = 2.5 \cdot 10^{-4}$ sec, indicating the effective mechanism by which the plasma sheds heat.

A high-speed time scan of the discharge spectrum showed that in the wavelength range $\lambda = (5-7) \cdot 10^{-4}$ mm the radiation spectrum of the discharge is continuous and uniform and its intensity decreases little over the time that the discharge burns. The results of the absolute spectral measurements give a magnitude of radiated energy close to the energy of an absolute black body at $T = 4500 \pm 300^\circ\text{K}$ in the indicated wavelength interval.

The V-A characteristics were measured for capillaries of different length, which permitted determining the magnitude of the total voltage jump near the electrode. The results of measurements in a series of 5-10 firings were averaged statistically. The magnitude of the total near-electrode jump on the capillary $l = 10$ mm long was 30% of the total voltage jump.

The average V-A characteristics on the capillaries of different diameters were analyzed in the coordinates $\langle\sigma\rangle(N)$ (the average conductivity of the discharge $\langle\sigma\rangle = I/\pi R^2 E$, the electrical power of the discharge $N = IE$, I is the discharge current, R is the radius of the capillary, and E is the intensity of the electric field).

The dependence $\langle\sigma\rangle(N)$ is shown in Fig. 4 together with an indication of the mean-square error for discharges with different diameters $p_0 = 10^8$ Pa [1) $d = 1.96$ mm, 2) $d = 1.026$ mm, 3) $d = 0.7$ mm], $p_0 = 5 \cdot 10^7$ Pa [4) $d = 1.96$ mm, 5) $d = 0.7$ mm], $p_0 = 2.5 \cdot 10^7$ Pa [6) $d = 1.06$ mm, 7) $d = 0.73$ mm, 8) $d = 1.84$ mm].

The following experimental facts indicate indirectly the uniformity of the composition of the plasma: coincidence of the V-A characteristics for quartz and sodium glass capillaries; closeness of the results in the $\langle\sigma\rangle(N)$ plane when the characteristic discharge time decreases from $\tau = 10^{-2}$ sec to $\tau = 10^{-3}$ sec; coincidence of the V-A characteristics with firings at different initial charging levels of the capacitor band.

The small pressure drop in the capillary and the low efflux velocity out of the capillary could indicate that the process is nearly quasistationary for times $\tau = 10^{-2} - 10^{-3}$ sec.

Since the effect of the wall will be smallest in discharges with maximum capillary diameters, it is interesting to estimate for them the temperature dependence of the electrical conductivity of a cesium plasma based on the stationary equation of heat conduction (Elenbass-Geller equation) and the equation for the total current:

$$\frac{1}{r} \frac{d}{dr} \left(\lambda r \frac{dT}{dr} \right) + \sigma E^2 = 0, \quad I = 2\pi E \int_0^R \sigma r dr,$$

where $\lambda = 5.3\epsilon l T^3$ (radiative thermal conductivity) and $\sigma = \sigma(T)$ (conductivity) are nonlinear functions of the temperature; ϵ is the Stefan-Boltzmann constant; and, l is the Rosseland mean free path length for radiation.

We solved the problem in a form that is the inverse of the traditional forms [5]: The dependence $\sigma(T)$ was found from the computed dependence $\lambda(T)$ with the boundary condition $T|_{r=R} = T_R$ at the wall of the discharge and with the total current strength I and electric field intensity E known from the measured V-A characteristics. The problem was solved by the method of successive approximations, using the step approximation according to [6].

Figure 5 shows the dependence $\sigma(T)$ obtained for pressures of $p = (4; 6; 10) \cdot 10^7$ Pa (curves 1-3, respectively). The quantitative agreement with theoretical data is satisfactory ($\sigma \approx 10^2 \Omega^{-1} \cdot \text{cm}^{-1}$) [7]. However, the qualitative temperature dependence is different from that predicted in [7], where the conductivity increases with decreasing temperature. The parameter of nonideality γ in our experiments passes through the values 0.3-1.

LITERATURE CITED

1. P. P. Kulik, V. M. Melnikov, V. A. Riabii, and M. A. Titov, "The electrical conductivity of dense, highly nonideal cesium plasma," in: Proc. Eleventh Intern. Conf. on Phenom. in Ionized Gases, Prague (1973).
2. I. S. Kulikov, Thermodynamic Dissociation of Compounds [in Russian], Metallurgiya, Moscow (1969).
3. S. I. Belov, M. I. Demidov, et al., "Reversible opaqueness of optical quartz appearing during contact with a dense plasma," Zh. Prikl. Spektrosk., 10, No. 3 (1969).
4. N. I. Kuznetsova and G. B. Lappo, "Optical properties of plasma of alkali metals lithium, sodium, and potassium," Teplofiz. Vys. Temp., 17, No. 1 (1979).
5. S. V. Dresvin (ed.), Physics and Technology of Low-Temperature Plasma [in Russian], Atomizdat, Moscow (1972).
6. M. E. Zarudi, "Methods for calculating the characteristics of an arc in a channel," Teplofiz. Vys. Temp., 6, No. 1 (1968).
7. E. E. Son and G. A. Pavlov, "Investigation of the electrical conductivity of a weakly nonideal plasma in a shock tube," Teplofiz. Vys. Temp., 9, No. 5 (1971).